The β Subunit Determines the Ligand Binding Properties of Synaptic Glycine Receptors

Joanna Grudzinska,[1] Rudolf Schemm,[1]
Svenja Haeger,[2] Annette Nicke,[1]
Guenther Schmalzing,[2] Heinrich Betz,[1,*]
and Bodo Laube[1]
[1]Department of Neurochemistry
Max-Planck-Institute for Brain Research
Deutschordenstrasse 46
D-60528 Frankfurt am Main
Germany
[2]Department of Molecular Pharmacology
Medical School of the Technical
   University of Aachen
Wendlingweg 2
D-52074 Aachen
Germany

Summary

Inhibitory glycine receptors (GlyRs) regulate motor coordination and sensory signal processing in spinal cord and other brain regions. GlyRs are pentameric proteins composed of membrane-spanning α and β subunits. Here, site-directed mutagenesis combined with homology modeling based on the crystal structure of the acetylcholine binding protein identified key ligand binding residues of recombinant homooligomeric α1 and heterooligomeric α1β GlyRs. This disclosed two highly conserved, oppositely charged residues located on adjacent subunit interfaces as being crucial for agonist binding. In addition, the β subunit was found to determine the ligand binding properties of heterooligomeric GlyRs. Expression of an α1β tandem construct and affinity purification of metabolically labeled GlyRs confirmed a subunit stoichiometry of 2α3β. Because the β subunit anchors GlyRs at synaptic sites, our results have important implications for the biosynthesis, clustering, and pharmacology of synaptic GlyRs.

Introduction

A precise balance between neuronal excitation and inhibition is crucial for proper functioning of the CNS. Disturbance of neuronal excitation-inhibition homeostasis results in severe pathological phenotypes, such as excitotoxic neurodegeneration, epilepsy, muscular spasticity, and mental retardation (Zoghbi et al., 2000). The amino acid glycine regulates neuronal activity by activating two classes of phylogenetically and structurally distinct ligand-gated ion channels, chloride-permeable inhibitory glycine receptors (GlyRs), which are members of the pentameric Cys-loop receptor superfamily, and cation-selective excitatory N-methyl-D-aspartate receptors (NMDARs), which belong to the tetrameric ionotropic glutamate receptor family (Cull-Candy et al., 2001; Grutter and Changeux, 2001). Both

receptor classes are crucially involved in brain function and malfunction, with their subunit compositions determining their specific functional properties and subcellular localizations (Cull-Candy et al., 2001; Laube et al., 2002).

GlyR-mediated synaptic inhibition in spinal cord and brain stem is essential for the control of motor rhythm generation, coordination of spinal reflex responses, and processing of sensory signals (Legendre, 2001). Synaptically localized GlyR proteins are composed of two types of homologous membrane-spanning subunits, the 48 kDa α and the 58 kDa β subunits (reviewed in Laube et al., 2002; Rajendra et al., 1997). Each subunit consists of a large extracellular binding domain, four transmembrane segments (M1–M4), and a long intracellular loop between M3 and M4. The α subunits are thought to contain major determinants of agonist and antagonist binding and exist in four different isoforms (α1–α4) encoded by regionally and developmentally distinctly expressed genes (Harvey et al., 2004; Malosio et al., 1991). The unique β subunit gene (Glrb) in contrast is transcribed at all developmental stages in many regions of the mammalian CNS (Fujita et al., 1991; Malosio et al., 1991). Upon heterologous expression, all α subunits generate functional homooligomeric GlyRs (Kuhse et al., 1995; Laube et al., 2002), which in vivo are found extrasynaptically (Singer and Berger, 2000; Takahashi et al., 1992). In contrast, the β subunit forms channels only upon coassembly with α subunits at an invariant stoichiometry (Bormann et al., 1993; Kuhse et al., 1993). A hydrophobic sequence within the M3–M4 loop of the β subunit interacts with the receptor-anchoring protein gephyrin (Meyer et al., 1995) and thereby provides for synaptic clustering of heterooligomeric GlyRs (Kneussel and Betz, 2000).

From cross-linking experiments with GlyR purified from spinal cord, the subunit stoichiometry of heterooligomeric GlyRs has been deduced to be 3α:2β (Langosch et al., 1988). Homo- and heterooligomeric GlyRs differ in chloride conductance (Bormann et al., 1993) and picrotoxinin sensitivity (Pribilla et al., 1992). UV cross-linking of the radiolabeled antagonist strychnine to GlyR purified from spinal cord produced a selective labeling of α subunits, consistent with only the α and not the β subunits contributing to ligand binding (Pfeiffer et al., 1982). Mutational analysis of homooligomeric α1 GlyRs revealed several residues important for agonist and/or antagonist interaction (reviewed in Breitinger and Becker, 2002; Laube et al., 2002; Rajendra et al., 1997). So far, an eventual contribution of the β subunit to ligand binding has not been investigated.

Structure-function studies on other members of the Cys-loop receptor family, such as nicotinic acetylcholine receptors (nAChRs), GABA$_A$ receptors (GABA$_A$Rs), and the 5-HT$_3$ receptor, indicate that ligand binding takes place at the interface between the N-terminal domains of two adjacent subunits (Corringer et al., 2000). This is consistent with crystallographic data on a homologous soluble acetylcholine binding protein (AChBP) from the snail *Lymnea stagnalis* (Brookhaven Protein
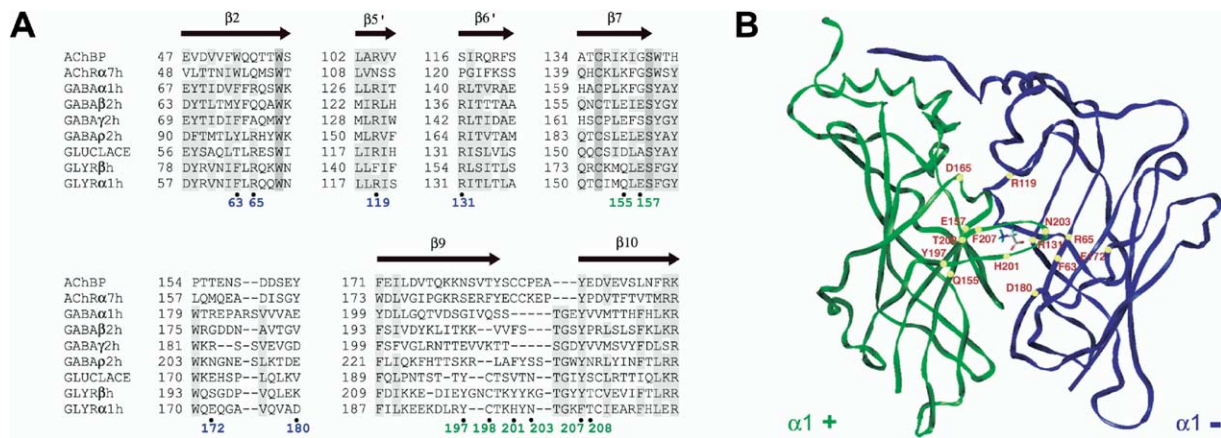
*Correspondence: neurochemie@mpih-frankfurt.mpg.de

Figure 1. Alignment and Structural Model of the Extracellular Domain of the Human GlyR α1 Subunit

(A) Partial sequence alignment of AChBP with the amino-terminal subdomains of the human GlyR α1 and β subunits, the human nAChR α7 subunit, the glutamate-gated chloride channel α subunit from *C. elegans* (GLUCLACE), and the human GABA$_A$R subunits α1, β2, γ2, and ρ2. Secondary structure elements found in AChBP are indicated above its sequence. Residues conserved throughout the superfamily are underlain in dark gray, and partially conserved residues are underlain in light gray. Residues mutated in the GlyR α1 subunit are numbered underneath the alignment. Amino acid residues located at the − side of the subunit interfaces are shown in blue, and residues located at the + side are shown in green.

(B) Model of the extracellular domains of two adjacent GlyR α1 subunits (side view). Backbones of the subunits are illustrated in ribbon representations (green, + side; blue, − side of the interface). Glycine was docked into the interface followed by energy minimization. Residues thought to contribute to ligand recognition (yellow dots) were mutated.

Data Bank entry 1I9B) (Brejc et al., 2001). In this pentameric protein, residues from both sides of the subunit interface contribute to ligand binding, with the plus (+) side presenting loop elements, and the minus (−) side presenting β sheets, toward the interface. Since the AChBP displays up to 27% amino acid identity to the extracellular N-terminal domains of Cys-loop family members, it has been used as template in modeling of nAChR (Le Novere et al., 2002), GABA$_A$R (Cromer et al., 2002), GlyR (Laube et al., 2002), and 5HT$_3$ receptor (Maksay et al., 2003) proteins.

In the present study, electrophysiological and molecular modeling techniques were combined to explore the ligand binding sites of homo- and heterooligomeric GlyRs. Based on the crystal structure of the AChBP, models of the N-terminal domains of the α1 and β subunit were generated. Amino acid residues predicted to participate in ligand binding were mutated to reveal key residues implicated in agonist and antagonist binding. In contrast to previous reports in which the GlyR β subunit was suggested to have mainly a structural role in anchoring the receptor at postsynaptic sites (see Kuhse et al., 1995), here a major role of the β subunit in ligand binding is demonstrated. Furthermore, expression of a tandem α1β construct along with metabolic labeling analyses of recombinant GlyRs discloses the β subunit as major component of heterooligomeric GlyR proteins and establishes a subunit stoichiometry of 2α1:3β. Finally, our results indicate a common mode of binding for the α-carboxylate and amino groups of amino acid neurotransmitters in different receptor families.

Results

Strategy for Mutational Analysis of the GlyR α1 Subunit

In order to identify ligand binding residues of the GlyR, the crystal structure of the AChBP (Brejc et al., 2001)

was taken as a template to generate a pentameric three-dimensional model of the extracellular N-terminal domain of the human α1 subunit (Laube et al., 2002). A partial alignment of the GlyR α1 subunit with the AChBP sequence as chosen for homology modeling is presented in Figure 1A; Figure 1B displays the modeled polypeptide backbones of two neighboring GlyR α1 subunits. The crystal structure of the AChBP was resolved with different ligands located in the binding pocket formed at subunit interfaces (Brejc et al., 2001; Celie et al., 2004). Therefore, we decided to examine the functional importance of residues homologous to the AChBP positions, which lie within close distance (≤6 Å) of the bound ligand and have been shown to contribute to ligand binding in different receptors of the Cys-loop family (Sixma and Smit, 2003). Specifically, we focused on the following charged and aromatic residues located either at the + side (α1Q155, α1E157, α1Y197, α1H201, α1F207, α1T208) or the − side (α1F63, α1R65, α1R119, α1R131, α1E172, α1D180) of the interface. Residues α1F159, α1K200, α1Y202, and α1T204, which were substituted previously (Rajendra et al., 1995; Schmieden et al., 1993; Vandenberg et al., 1992b), were excluded from our analysis. All amino acid side chains listed above were exchanged to alanine, except for glutamate 157, which was mutated to aspartate, since introduction of an alanine at this position results in a nonfunctional receptor (Laube et al., 2000). Additionally, α1R65, α1R119, and α1R131 were isofunctionally replaced by lysine. The positions of the substitutions made are indicated in Figure 1B.

Agonist Response Properties of Homomeric Mutant α1 GlyRs

First, we examined whether the mutations that were introduced change agonist activation of the homooligomeric α1 GlyR expressed in *Xenopus laevis* oocytes. All

Table 1. Agonist and Antagonist Response Properties of Homooligomeric α1 GlyRs

cRNA Injected	Glycine		Taurine		Strychnine
	EC_{50} [mM] (n)	n_H	EC_{50} [mM] (n)	I_{max}tau/I_{max}gly (%)	IC_{50} [nM] (n)
α1 wt	0.19 ± 0.05 (12)	2.4 ± 0.8	3.6 ± 1.6 (10)	25 ± 9	36 ± 10 (9)
α1F63A	≥250* (6)	ND	≥300* (4)	20 ± 5	12000 ± 3000* (5)
α1R65K	41 ± 12* (5)	2.0 ± 0.3	58 ± 21* (5)	54 ± 7*	170 ± 80* (6)
α1R65A	≥250* (4)	2.2 ± 0.4	84 ± 20* (6)	83 ± 19*	160 ± 50* (4)
α1R119K	11 ± 4.1* (7)	1.8 ± 0.3	25 ± 19* (7)	37 ± 15	130 ± 70* (6)
α1R119A	27 ± 12* (5)	1.9 ± 0.1	67 ± 29* (7)	7.0 ± 1.0*	250 ± 120* (4)
α1R131K	2.3 ± 1.7* (5)	0.9 ± 0.2*	3.6 ± 1.8 (5)	57 ± 16*	830 ± 400* (6)
α1R131A	0.11 ± 0.09 (8)	1.6 ± 0.4	0.42 ± 0.16* (6)	65 ± 10*	13000 ± 3600* (8)
α1Q155A	2.5 ± 0.9* (9)	1.5 ± 0.3*	26 ± 5* (5)	26 ± 15	69 ± 23* (6)
α1E157D	≥250* (5)	ND	≥300* (5)	96 ± 6*	NI (5)
α1E172A	0.46 ± 0.33 (7)	1.9 ± 0.6	6.9 ± 0.9* (8)	31 ± 11	23 ± 12 (7)
α1D180A	0.49 ± 0.28* (7)	2.4 ± 0.4	6.0 ± 1.2 (5)	30 ± 11	26 ± 15 (7)
α1Y197A	0.45 ± 0.14* (6)	2.0 ± 0.9	4.9 ± 2.9 (5)	31 ± 17	37 ± 7 (7)
α1H201A	0.27 ± 0.16 (8)	2.1 ± 0.4	ND	ND	69 ± 40 (7)
α1N203A	0.83 ± 0.21* (8)	2.5 ± 0.5	5.7 ± 1.7 (6)	42 ± 21	32 ± 18 (7)
α1F207A	≥250* (8)	ND	ND	ND	NI (4)
α1T208A	0.69 ± 0.25* (8)	1.7 ± 0.3	5.7 ± 1.5 (4)	58 ± 15*	2200 ± 800* (7)

All values are given as means ± SD. Asterisks indicate values that are significantly different (p < 0.01) from wt (Student's t test). ND, not determined; NI, no inhibition; n, number of experiments.

α1 mutants generated functional receptors, with maximal glycine-induced current (I_{max}) values in the range of 50–220 nA/mV, except α1E157D and α1F207A, which produced low-current responses in the range of 10 nA/mV even after application of 300 mM glycine. Wild-type (wt) α1 GlyRs displayed a glycine EC_{50} value of 0.19 ± 0.05 mM (Table 1). Substitutions of the arginine residues α1R65 and α1R119 caused dramatic reductions in apparent glycine affinity even upon isofunctional replacement (60- to 1300-fold; see Figure 2A). In the case of the substitutions α1F63A, α1R65A, α1E157D, and α1F207A, the EC_{50} value could only be estimated to be ≥250 mM (Table 1), because glycine concentrations up to 300 mM failed to saturate the current response. In contrast, the following mutations had only small or no effects on the dose response: αR131K and -A, α1Q155A, α1E172A, α1D180A, α1Y197A, α1H201A, and α1T208A. EC_{50} values were increased at most by 2- to 10-fold as compared to the wt α1 GlyR. This is consistent with these amino acid residues playing only minor roles in agonist binding and/or receptor function.

In addition to the full agonist glycine, we also tested the partial agonist taurine. Mutants that showed only low expression or had no effect on apparent glycine affinity (α1H201A and α1F207A) were excluded from analysis. All substitutions that affected the EC_{50} value of glycine also reduced that of taurine (Table 1), indicating that the same amino acid residues are essential for the binding of both agonists. To evaluate whether the α1 subunit mutations introduced also might affect receptor gating, activation by the partial agonist taurine was compared to that seen with the full agonist glycine (I_{max}tau/I_{max}gly; see Table 1). Taurine is a low-efficacy agonist; therefore, changes in gating properties should become apparent as a reduction in the relative maximal inducible current (Colquhoun, 1998). Except for α1R119A, all mutations examined showed a similar or even higher relative maximal current with taurine than the wt α1 GlyR (Table 1). Based on the theoretical analysis of the interdependence of binding and gating in receptor activation (Colquhoun, 1998), this indicates

that mainly binding rather than gating mutants were generated here.

Evaluation of Residues Important for Antagonist Interaction

To determine whether the α1 residues mutated also contribute to antagonist binding, inhibition curves for strychnine were recorded. Strychnine is a competitive antagonist of the GlyR, with an IC_{50} value of 36 ± 10 nM at wt α1 GlyRs. Six out of 16 of the amino acid substitutions tested changed the IC_{50} value of strychnine >10-fold (Table 1 and Figure 2B). The mutations α1E157D and α1F207A produced strychnine-insensitive GlyRs that were not inhibited even at rather high strychnine concentrations (≤500 μM). A strongly reduced inhibition by strychnine (330-fold) was also observed for the α1F63A replacement. Of the arginine substitutions examined, only the α1R131 mutations caused a marked increase in the IC_{50} value of strychnine, with a 20-fold change upon lysine and a 360-fold change upon alanine incorporation. In contrast, the α1R65 and α1R119 mutations had only minor effects on strychnine inhibition (4- to 7-fold reduction). Another substitution affecting strychnine binding is α1T208A, which led to a 60-fold shift in IC_{50} value. Together, these results indicate that within the binding pocket strychnine interacts with several of the residues required for glycine binding.

Model of the Binding Pocket of the Homooligomeric GlyR

From our previous model of the α1 GlyR binding pocket, several residues located at the interface of two adjacent α1 subunits had been suggested to contribute to glycine binding (Laube et al., 2002). Specifically, three arginines located on the – side (α1R65, α1R119, and α1R131) and five residues on the + side (α1Q155, α1E157, α1Y197, α1H201, and α1F207) appeared to be good candidates for interactions with the α-carboxyl and α-amino groups of the agonist. Considering previously described effects of α1 substitutions on glycine
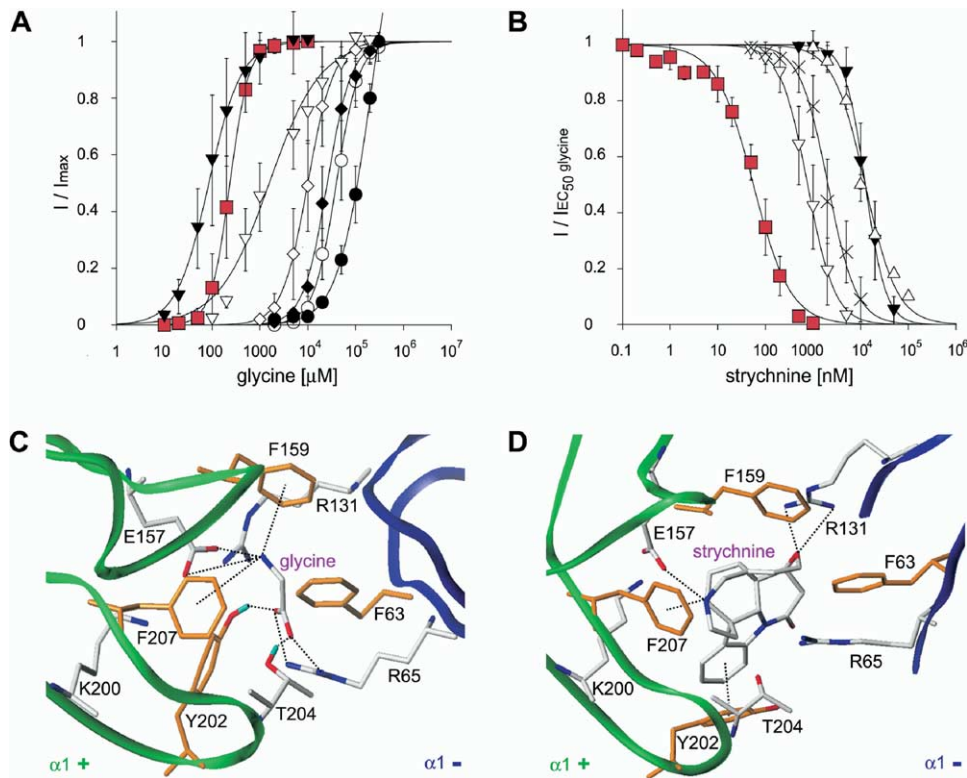
Figure 2. Glycine Responses and Strychnine Inhibition of Homopentameric wt and Mutant α1 GlyRs and Deduced Ligand Docking Models

In vitro transcribed wt or mutant α1 cRNAs were injected into *Xenopus laevis* oocytes. Membrane currents elicited by superfusion of increasing glycine concentrations were recorded after 1–2 days. Data points represent means ± SD (bars shown when larger than symbols) from 4 to 12 experiments, normalized to the corresponding I_{max} or, in the case of inhibition curves, I_{EC50} of glycine. (A) Glycine dose responses recorded from wt α1 (red squares) and mutant α1R65K (white circles), α1R65A (black circles), α1R119K (white diamonds), α1R119A (black diamonds), α1R131K (downward-pointing white triangles), and α1R131A (downward-pointing black triangles) GlyRs. (B) Strychnine inhibition curves obtained with oocytes injected with wt α1 (red squares) and mutant α1F63A (upward-pointing white triangles), α1R131K (downward-pointing white triangles), α1R131A (downward-pointing black triangles), and α1T208A (Xs) cRNAs. Data are plotted as a fraction of the glycine current elicited in the absence of strychnine. (C) Model of glycine binding at the interface of two adjacent GlyR α1 subunits. The α-carboxyl group is ligated by the positively charged α1R65 on the − side and builds hydrogen bonds with α1T204 and α1Y202 on the + side of the interface. On the + side, the α-amino group is stabilized by the γ-carboxyl group of α1E157 and via cation-π interactions with α1F159 and α1F207. (D) Close-up view of the modeled α1 binding pocket docked with strychnine. The guanidinium group of α1R131 interacts with oxygen O24 of strychnine, and the protonated nitrogen N19 points toward α1E157. This positive charge is further stabilized via a cation-π interaction with α1F207; α1Y202 stabilizes strychnine's aromatic ring. In (C) and (D), the backbones of the α1 subunits are illustrated in a ribbon representation (green, + side; blue, − side) and are only partially shown when overlapping with residues. Key residues are highlighted by a stick representation, in which white sticks represent carbon atoms, red sticks represent oxygen atoms, and blue sticks represent nitrogen atoms. Aromatic residues lining the binding pocket are depicted in orange. The aromatic side chains α1F63 and α1F159 stabilize the guanidinium groups of α1R65 and α1R131, respectively. Main interactions with the ligands are further indicated by dashed lines. Note that both binding pockets are not presented in exactly the same orientation to enable the best view on receptor ligand interactions.

and strychnine affinity (Laube et al., 2000; Rajendra et al., 1995; Schmieden et al., 1993; Vandenberg et al., 1992a; Vandenberg et al., 1992b), we generated a refined three-dimensional model of the ligand binding site of the α1 GlyR. Glycine was docked into the binding pocket followed by several energy minimization runs (for details, see Experimental Procedures). In the lowest-energy docking mode, glycine's α-carboxyl group was orientated toward the +, and the α-amino group toward the −, sides of the binding pocket. Residues α1F63, α1R65, α1E157, α1F207 (this study), α1F159, α1K200, α1Y202, and α1T204 (Rajendra et al., 1995; Schmieden et al., 1993; Vandenberg et al., 1992b), whose mutation severely affects the glycine EC₅₀ value (55- to 8600-fold), were assumed to contribute to ago-

nist binding. Figure 2C shows this model with glycine computationally docked into the binding site. The main conclusion resulting from this improved model is that glycine bridges the interface of adjacent subunits via its α-amino and α-carboxyl groups by mainly interacting with two oppositely charged side chains at the + (α1E157) and − (α1R65) sides, respectively (Figure 2C). Consistent with this mode of binding, the effects of the isofunctional mutations α1R65K and α1E157D on the glycine EC₅₀ value were smaller than those with the respective alanine substitutions, indicating that the α-carboxyl and α-amino groups of glycine are ionically paired with these residues. The increased efficacy at mutation α1E157D of the partial agonist taurine (Table 1), which has a longer main chain that compensates

that of the reduced side chain length of the introduced aspartate, is also in accordance with a crucial role of α1E157 in directly ligating agonists. The α-carboxyl group of glycine further interacts via two additional H-bridges with the hydroxyl groups of α1Y202 and α1T204; hence, glycine binding is strongly reduced upon the substitutions α1Y202F (Rajendra et al., 1995) and α1T204A (Rajendra et al., 1995; Vandenberg et al., 1992b). Two cation-π interactions with the aromatic side chains of α1F159 and α1F207 are predicted to stabilize the α-amino group of glycine (Figure 2C). Indeed, the isofunctional substitutions α1F159Y and α1F207Y have been shown to increase or to not affect apparent glycine binding affinities (Laube et al., 2000; Schmieden et al., 1993), whereas alanine substitutions at these positions nearly abolished glycine binding (this study; and B.L., unpublished data). The proper side chain orientations of the crucial residues α1R65 and α1E157 are predicted to be stabilized by additional cation-π interactions with α1F63 and α1Y202, and by a salt bridge with α1K200, respectively (Figure 2C).

Using computational docking, we also identified specific interactions for the antagonist strychnine within the binding pocket (Figure 2D). In contrast to glycine binding, strychnine binding is most strongly affected upon substitution of α1R131, whereas substitutions of α1R65 have only a modest effect. We therefore propose that the oxygen at position 24 of strychnine directly interacts with the guanidinium group of α1R131. The positively charged N19 of strychnine, which is protonated at physiological pH (Becker, 1992), mainly interacts with the negatively charged side chain of α1E157 and is also stabilized by cation-π interactions with α1F159 and α1F207. An additional important interaction exists between the benzene ring of strychnine and the aromatic side chain of α1Y202, which are likely to form a π-π bond. Interestingly, in contrast to what is found for glycine binding, loss of the hydroxyl group of α1Y202 in the α1Y202F mutation does not affect strychnine binding (Rajendra et al., 1995), consistent with a pure π-π interaction as predicted from our model. Notably, major differences in the orientation of side chains or in the overall structure of the backbone are not detectable between the glycine- and the strychnine-ligated binding pockets. Only residue α1Y202 is pushed toward the outside of the pocket upon strychnine binding, resulting in a more open conformation of the second Cys-loop. The interactions of α1F63 with α1R65, and of α1K200 with α1E157, are maintained in the strychnine bound model, similar to the situation obtained after glycine binding. In summary, our model allows us to dock agonists and antagonists into the binding site located at the intersubunit crevice in orientations consistent with our mutational data. However, a pronounced reorientation of a side chain emerges only in a single case, α1Y202.

Rescue of Mutant α1 GlyRs by Coexpression with a wt β Subunit
In the adult spinal cord, synaptic GlyRs consist of α and β subunits. The glycine EC_{50} value of the heterooligomeric α1β wt receptor is known to be similar to that of homooligomeric α1 GlyRs (Kuhse et al., 1993).

To evaluate whether the β subunit also contributes to ligand binding, we expressed the low-affinity α1R65A and the α1E157D mutants together with the wt β subunit. For heterooligomeric GlyR expression, α1 and β cRNAs were mixed at a ratio of 1:4 to minimize generation of homopentameric α1 receptors. Surprisingly, the β subunit was able to rescue the dramatic increase in glycine EC_{50} value caused by the α1 substitutions (Figure 3A) to nearly α1β wt levels (Table 2). In contrast to the homooligomeric α1R65A and α1E157D GlyRs, which both displayed no current saturation at 300 mM glycine (EC_{50} values $\geq$ 250 mM; see Table 1), the heterooligomeric α1R65Aβ and α1E157Dβ receptors showed maximal currents already at 5–10 mM glycine. Most astonishing was the rescue for the α1E157D mutant, which gave only small currents as a homopentamer but full current flow upon coexpression with the β subunit (Figure 3A). Moreover, coexpression of the α1R65A mutant with the β subunit resulted in a heterooligomeric receptor with a glycine EC_{50} of 0.65 ± 0.13 mM, i.e., a value that was not significantly different from that of wt α1β GlyRs (EC_{50} of glycine 0.48 ± 0.15 mM). Similar results were obtained when the α1E157D mutant was coexpressed with the wt β subunit (EC_{50} value 0.83 ± 0.26 mM) (Figure 3B). Thus, the overall rescue effects of the β subunit on apparent glycine affinity were 380-fold and 300-fold for the α1R65A and α1E157D substitutions, respectively. These results indicate that the β subunit has a dominant role in agonist binding to heterooligomeric GlyRs.

To examine whether the β subunit is also able to rescue strychnine binding to mutant α1 subunits, we coexpressed the wt β subunit with α1 mutants that displayed strongly reduced strychnine affinities (α1R131Aβ and α1E157Dβ). These substitutions are located at the – and + sides of the interface, respectively. At wt homo- and heterooligomeric GlyRs, strychnine IC_{50} values are almost identical (α1, IC_{50} = 36 ± 10 nM and α1β, IC_{50} = 32 ± 8 nM; see Tables 1 and 2). Interestingly, upon coexpression with the β subunit only α1E157D was rescued to wt levels (IC_{50} = 35 ± 10 nM), whereas the α1R131Aβ GlyR retained a strongly reduced strychnine affinity (IC_{50} = 20000 ± 4000 nM) (Figure 3C), although its glycine response was comparable to that of wt α1β GlyRs (see Table 1). These results suggest a differential contribution of subunit interfaces to strychnine binding at heterooligomeric α1β GlyRs.

β Subunit Residues Implicated in Ligand Binding
To further investigate the role of the β subunit in ligand binding, we replaced residues of the β subunit (βR86, βR154, βE180, βK223, βY225, βK226, βY231) by alanine, which are homologous to the ligand binding residues of the α1 subunit (α1R65, α1R131, α1E157, α1K200, α1Y202, α1N203, α1F207, respectively). Then, mutant β and wt α1 cRNAs were coinjected at a ratio of 4:1. To distinguish between homo- and heteromeric receptors, all glycine dose-response curves were recorded in the presence of 100 μM picrotoxinin, which inhibits homo- but not heteropentameric GlyRs (Pribilla et al., 1992). Most of the mutant β subunits generated heterooligomeric receptors with reduced apparent glycine affinities (Figure 4A and Table 2). Particularly prominent increases
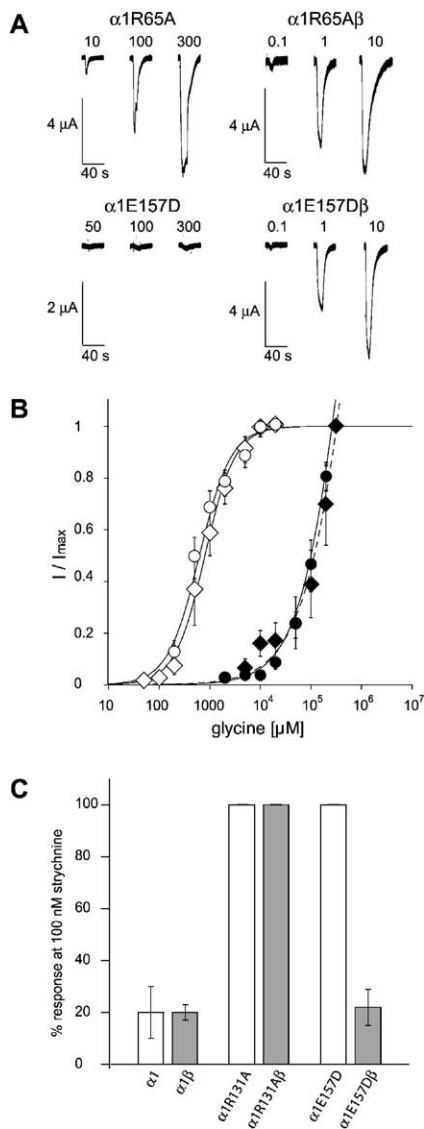
Figure 3. Rescue of α1 Mutant GlyRs by Coexpression with the wt β Subunit

(A) Glycine responses of homo- and heterooligomeric GlyRs. Homopentameric α1R65A and α1E157D GlyRs show no current saturation at 300 mM glycine, and current flow is strongly reduced for the α1E157D substitution. Upon coexpression of both mutant α1 and the wt β subunit, glycine responses are rescued to almost wt levels, with current saturation occurring at 5–10 mM glycine. Note that current flow is also restored with the α1E157Dβ mutant. Agonist concentrations are given in mM.

(B) Glycine dose-response curves for homooligomeric α1R65A (black circles) and α1E157D (black diamonds) receptors, and heterooligomeric α1R65Aβ (white circles) and α1E157Dβ (white diamonds) receptors. Note leftward shift of glycine dose-response curves with both heterooligomeric receptors. Data points represent means ± SD (shown when larger than symbols) from six experiments, normalized to the corresponding I_{max} of glycine.

(C) Strychnine inhibition of wt and mutant α1 (white bars) and α1β (gray bars) GlyRs. Glycine was applied at the corresponding EC_{50} value, and inhibition by 100 nM strychnine was determined. Data are presented as means ± SD. Note that coexpression of the β subunit rescues strychnine inhibition only for the α1E157D but not the α1R131A subunit.

in glycine EC_{50} value were obtained for α1βR86A and α1βE180A GlyRs (EC_{50} = 5.7 ± 2.1 mM and 2 ± 0.7 mM, respectively). More modest changes in the glycine EC_{50} value (2- to 3-fold) were observed with the following mutant receptors: α1βR154A, α1βK223A, α1βY225A, and α1βY231A. In contrast, the βK226A substitution had no significant effect on apparent glycine affinity. Since βR86 and βE180 are homologous to α1R65 and α1E157, our results highlight the importance of these charged side chains for agonist binding to both homo- and heterooligomeric GlyRs. Furthermore, they underline the important contribution of the β subunit to ligand binding in α1β receptors.

We also examined strychnine antagonism with the heterooligomeric mutant GlyRs. Substitutions α1βE180A, α1βK223A, and α1βY225A resulted in significant reductions of the IC_{50} value of strychnine (3- to 6-fold). In contrast, the α1βR154A, α1βK226A, and α1βY231A GlyRs displayed no detectable changes in antagonist affinity, with IC_{50} values similar to wt (Figure 4B and Table 2). These results suggest that the β subunit of the GlyR is important for both agonist and antagonist binding.

Models of the Heterooligomeric Subunit Interfaces
For generating models of the heterooligomeric subunit interfaces, one α1 subunit of the α1α1 dimer (Figure 1B) was replaced by a β subunit either on the + or the − side, thereby creating α1β and βα1 interfaces, respectively. Since all residues crucial for ligand binding to the α1 subunit are conserved in the β polypeptide, we assumed that homologous residues in both subunits are involved in ligand binding. Modeling of the heteromeric interfaces revealed that the α-carboxyl and α-amino groups of glycine are consistently stabilized via ionic interactions with the β residues R86 at the α1β (data not shown) and E180 at the βα1 (Figure 4C) interfaces, respectively. Hence, the heterooligomeric interfaces bind the amino and the carboxyl group of glycine through the combinations α1E157/βR86 and βE180/α1R65 of the α1β or βα1 dimers, respectively. Further stabilization may be provided by the + side residues α1F159, α1K200, α1Y202, α1T204, and α1F207 at the α1β interface and by the homologous β side chains βF182, βK223, βY225A, βT228, and βY231 at the βα1 interface. This is consistent with the results obtained in this study, where substitutions of βR86 (homologous to α1R65) at the − side of the binding pocket, and of βE180 (homologous to α1E157) at the corresponding + side, caused increases in the glycine EC_{50} value of the heterooligomeric GlyR. Because the enthalpies calculated for glycine binding to both interfaces are very similar (ΔH = −19.6 kcal/mol [α1β] versus ΔH = −19.2 [βα1] kcal/mol), we suppose that glycine binds with similar affinity at both interfaces. This assumption is consistent with both the rescue of α1 binding site substitutions seen upon coexpression of the wt β subunit and the increased glycine EC_{50} values found for substitution of β residues at both the + and − sides of subunit interfaces. Notably, the effects of β subunit substitutions on strychnine inhibition are different. Here, coexpression of the β subunit rescued strychnine binding only in case of α1 substitutions that are located at the + side, indicating a preferential binding of strychnine to the βα1

Table 2. Agonist and Antagonist Response Properties of Heterooligomeric α1β GlyRs

| cRNA Injected | Glycine | | Strychnine |
	EC$_{50}$ [mM] (n)	n$_H$	IC$_{50}$ [nM] (n)
wt α1β	0.48 ± 0.15 (8)	1.5 ± 0.2	32 ± 8 (5)
α1R65Aβ	0.65 ± 0.13 (6)	1.5 ± 0.2	ND
α1R131Aβ	0.57 ± 0.20 (5)	1.0 ± 0.3*	20000 ± 4000* (6)
α1E157Dβ	0.83 ± 0.26* (6)	1.5 ± 0.1	35 ± 10 (5)
α1βR86A	5.7 ± 2.1* (6)	1.0 ± 0.2*	ND
α1βR154A	0.93 ± 0.23* (8)	1.5 ± 0.2	27 ± 9 (5)
α1βE180A	2.0 ± 0.8* (9)	1.1 ± 0.3*	210 ± 60* (5)
α1βK223A	1.2 ± 0.3* (7)	1.6 ± 0.1	100 ± 14* (4)
α1βY225A	1.6 ± 0.5* (5)	1.5 ± 0.4	200 ± 30* (4)
α1βK226A	0.7 ± 0.2 (5)	1.5 ± 0.2	23 ± 9 (4)
α1βY231A	1.0 ± 0.2* (6)	1.3 ± 0.2	28 ± 16 (4)
(α1β)$_T$	NF (20)	—	ND
(α1β)$_T$ + α1E157D	≥ 250* (6)	ND	ND
(α1β)$_T$ + α1R65A	≥ 250* (6)	2.7 ± 0.5*	ND
(α1β)$_T$ + β	0.56 ± 0.22 (13)	1.6 ± 0.4	ND

Data are presented as means ± SD and marked with an asterisk when significantly different (p < 0.01) from wt receptors (Student's t test). ND, not determined; NF, not functional; n, number of experiments.
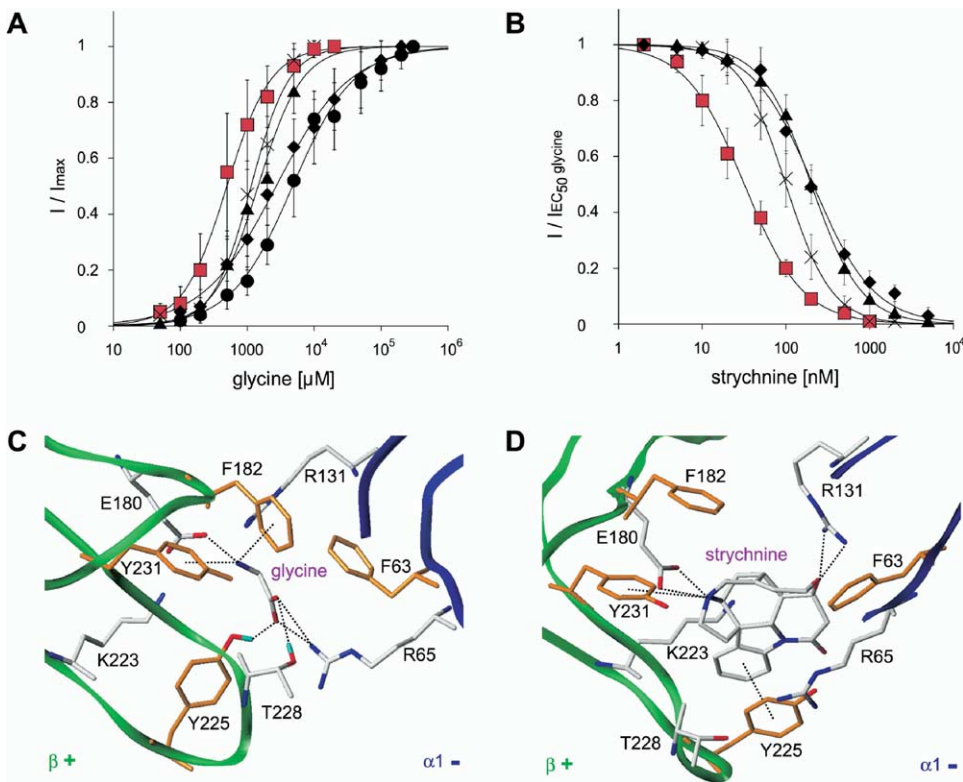

Figure 4. Glycine Responses and Strychnine Inhibition of Heterooligomeric GlyRs Containing Mutant β Subunits

(A) Glycine dose-response curves for wt α1β (red squares), α1βR86A (black circles), α1βE180A (black diamonds), α1βK223A (Xs), and α1βY225A (upward-pointing black triangles) GlyRs.

(B) Strychnine inhibition curves for wt α1β (red squares) and the mutant α1βE180A (black diamonds), α1βK223A (Xs), and α1βY225A (upward-pointing black triangles) GlyRs. Data points represent means ± SD (bars shown when larger than symbols) from four to five experiments, normalized to the corresponding I$_{max}$ or, in the case of inhibition curves, I$_{EC50}$ of glycine.

(C) Model of the heterooligomeric βα1 interface docked with the agonist glycine. Glycine interacts with βE180 at the + side, and α1R65 at the − side, of the binding pocket. Additional stabilization is provided by the hydrogen bonds with βY225 and βT228 located on the − side, and βF182 and βY231 on the + side, of the interface.

(D) Model of the βα1 interface ligated with strychnine. On the + side, the side chains of βE180, βK223, βY225, and βY231 interact with strychnine. On the − side, residue α1R131 stabilizes the antagonist. Note similarity of docking modes shown in (C) and (D) to those presented for α1 GlyRs in Figures 2C and 2D.

interface (Figure 4D). This is consistent with β subunit mutations not affecting strychnine potency when introduced at the – side and is also in agreement with our enthalpy calculations, which predict that strychnine binding at the $\alpha1\alpha1$ and $\beta\alpha1$ interfaces ($\Delta H = -38.2$ and -41.6 kcal/mol, respectively) is energetically favored to binding at the $\alpha1\beta$ interface ($\Delta H = -28.1$ kcal/mol).

Stoichiometry of Heterooligomeric $\alpha1\beta$ GlyRs

The heterooligomeric GlyR is thought to be composed of three $\alpha1$ and two β subunits (Langosch et al., 1988). However, when comparing the glycine EC$_{50}$ values of heterooligomeric receptors that carried mutations of homologous ligand binding residues in either the $\alpha1$ or the β subunit, we realized that homologous substitutions in the two subunits differentially affected the glycine response. Specifically, the $\alpha1$R65A substitution caused an increase in glycine EC$_{50}$ value (0.65 ± 0.13 mM) that was significantly smaller than that found for the homologous βR86A mutation (EC$_{50} = 5.7 \pm 2.1$ mM) (Table 2), suggesting that the β subunit determines agonist affinities. To unravel whether this reflects a higher copy number of β versus α subunits, we generated a concatemeric subunit fusion protein, in which the C terminus of the $\alpha1$ subunit was linked to the N terminus of the β subunit via a 7-fold alanine-glycine-serine repeat. Expression of this tandem construct $(\alpha\beta)_T$ in oocytes alone gave no significant current flow (Figure 5A). Furthermore, coexpression of the concatemeric subunit with mutant $\alpha1$ subunits ($\alpha1$R65A and $\alpha1$E157D) generated channels with pharmacological properties characteristic of homooligomeric $\alpha1$ receptors (Table 2), e.g., glycine EC$_{50}$ values similar to those of $\alpha1$R65A and $\alpha1$E157D homomeric GlyRs (see Table 1). In contrast, coexpression of $(\alpha\beta)_T$ with the wt β subunit resulted in a functional receptor with an EC$_{50}$ of 0.56 ± 0.22 mM (Table 2), i.e., a value identical to that of wt $\alpha1\beta$ GlyRs (EC$_{50} = 0.48 \pm 0.15$ mM). This is consistent with the subunit stoichiometry of the heterooligomeric GlyR being $2\alpha1{:}3\beta$.

To further establish the subunit composition of heterooligomeric GlyRs by an independent biochemical approach, we metabolically labeled $\alpha1\beta$ receptors with [^{35}S]methionine by coexpressing the $\alpha1$ subunit with a His-tagged β subunit. The radiolabeled GlyRs were then purified by metal affinity chromatography from digitonin extracts of the oocytes and analyzed by reducing SDS-PAGE (Sadtler et al., 2003). Figure 5B shows the ^{35}S-labeled subunit bands visualized by phosphorimaging. Quantification revealed that the coisolated nontagged $\alpha1$ subunit band contained 1.38-fold more radioactivity than the His-tagged β polypeptide (Figure 5B). This ratio is very close to the theoretical value of 1.42 calculated for a stoichiometry of $2\alpha1{:}3\beta$ subunits, based on 17 and 8 methionine residues per mature $\alpha1$ and β subunit, respectively ($\alpha1/\beta = 34 \times M/24 \times M$). To display the entire amounts of $\alpha1$ and β subunits synthesized from an injected 5-fold excess of β over $\alpha1$ cRNAs, we also coexpressed and purified His-tagged versions of both subunits. Quantification yielded a similar ratio of 1.35 of $\alpha1$ to β subunit radioactivities (data not shown). The almost identical ratios obtained by both protocols suggested that all recombinant $\alpha1$ sub-
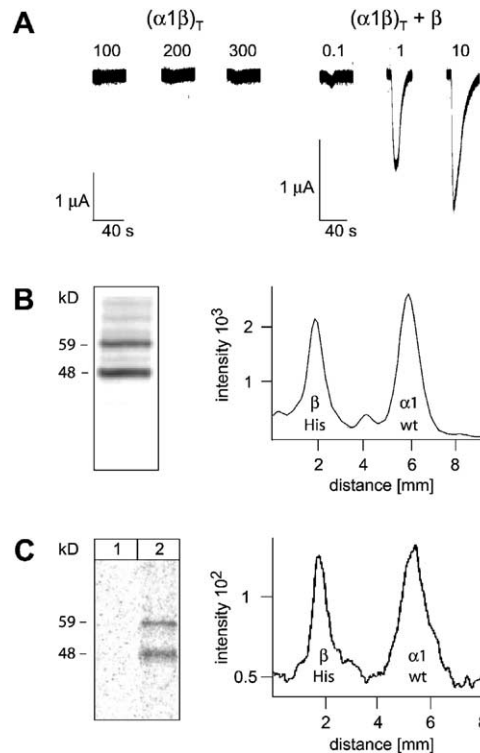

Figure 5. Subunit Stoichiometry of the Heterooligomeric GlyR

(A) Glycine currents recorded from oocytes expressing the tandem subunit $(\alpha\beta)_T$ either alone or together with the wt β subunit. Note lack of current responses in $(\alpha\beta)_T$ singly but not β coexpressing oocytes. Glycine concentrations are indicated in mM.

(B) Metabolic labeling of $\alpha1\beta$ GlyRs. *Xenopus* oocytes coexpressing a His-tagged β with a nontagged $\alpha1$ subunit were metabolically labeled with [^{35}S]methionine. Recombinant GlyRs were purified from oocyte extracts on Ni^{2+}-NTA Agarose and subjected to SDS-PAGE. Gel lanes were scanned with a PhosphoImager (left, with respective molecular masses of the GlyR subunits), and the relative ratio of the $\alpha1$ to β subunit radioactivity was determined (1.38).

(C) Surface labeling of heterooligomeric $\alpha1\beta$ GlyRs. *Xenopus* oocytes coexpressing metabolically labeled His-tagged β and nontagged $\alpha1$ subunits were surface labeled with biotin. Receptor complexes were isolated from a digitonin extract of ten pooled oocytes by Ni^{2+}-NTA Agarose and streptavidin bead chromatography and subjected to SDS-PAGE (left, lane 2). Nonbiotinylated oocytes showed no labeling (left, lane 1). Quantification of ^{35}S-labeled radioactivities revealed that the coisolated nontagged $\alpha1$ subunit contained 1.44-fold more radioactivity than the His-tagged β polypeptide (right).

units were associated with β subunits under the experimental conditions used. Moreover, these results further support an $2\alpha1{:}3\beta$ subunit stoichiometry of heterooligomeric GlyRs.

To exclude the possibility that intracellularly retained unassembled or partially assembled GlyR subunits might contribute to the above determined $\alpha1/\beta$ subunit ratios, we also purified metabolically labeled GlyRs from the cell surface. In oocytes, GlyRs have been shown to reach the plasma membrane only when fully assembled into functional channels (Büttner et al., 2001) and to be internalized as pentamers upon ubiquitination (Sadtler et al., 2003). Intact oocytes expressing metabolically labeled $\alpha1$ and His-tagged β subunits were therefore surface labeled with biotin, and GlyRs

were purified from digitonin extracts of ten pooled cells by sequential Ni^{2+}-NTA Agarose and streptavidin bead chromatography. After SDS-PAGE, quantification of ^{35}S-radioactivities in the subunit bands by phosphorimaging again resulted in an α1/β ratio of 1.44 (Figure 5C). We therefore conclude that the α1 and β GlyR subunits assemble at an invariant stoichiometry of 2α1:3β.

Discussion

In this study, we present a detailed mutational analysis of amino acid residues implicated in ligand binding to homo- and heterooligomeric GlyRs. Our data show that two conserved, oppositely charged residues located at the + and − sides of GlyR subunit interfaces (R65 and E157 in α1, R86 and E180 in β) provide the key ionic interactions with the α-amino and α-carboxylate groups of bound glycine. In addition, our results disclose a role of the β subunit in agonist binding to heterooligomeric GlyRs by demonstrating rescue of low-affinity α1 subunit binding mutants upon coexpression with the "structural" β polypeptide. These rescue experiments as well as our analysis of a tandem α1β construct and metabolic labeling of the recombinant α1β GlyR are consistent with a 2α1:3β subunit stoichiometry of heterooligomeric GlyRs. Our results imply that the β subunit is the predominant ligand binding subunit of synaptic GlyRs.

Conserved Amino Acid Binding Mode in Ligand-Gated Ion Channels

In all members of the Cys-loop receptor family, neurotransmitter binding is believed to require several discontinuous segments of the N-terminal extracellular regions of two adjacent subunits, which lie at the interface ∼30 Å from the membrane (Brejc et al., 2001; Unwin, 2003). Our mutational analysis of homo- and heterooligomeric GlyRs is consistent with this concept. Here, we show that ionic interactions at the interface of adjacent α, or α and β, subunits are crucial for stabilizing glycine's α-carboxyl and α-amino groups. Specifically, substitution of a conserved arginine residue at the − side of the binding pocket (R65 in the α1, R86 in the β subunit) caused drastic increases in the EC$_{50}$ value of glycine. At the corresponding + side, mutation of the conserved glutamate (E157 in α1, E180 in β) similarly led to drastic reductions in apparent glycine affinity. The effects of isofunctional replacements (α1R65K and α1E157D) were less marked, consistent with charged head groups at these positions being required for glycine binding. Furthermore, the efficacy of the partial agonist taurine was increased at the α1E157D substitution. Apparently, the larger intercharge distance in taurine compensated for the reduced side chain length of aspartate.

The importance of the binding residues identified here is further underlined by site-directed mutagenesis experiments on other Cys-loop receptors (reviewed in Sixma and Smit, 2003). The crucial residues α1R65 at the − side, and α1E157 at the + side, of the GlyR α1 subunit interface are conserved not only in GlyR proteins but also at the agonist binding interfaces formed

by α, β, and ρ subunits of the GABA$_{A/C}$R family (Figure 1A), where they provide key ionic interactions with the α-carboxylate and γ-amino groups of bound GABA (Cromer et al., 2002). Hence, these residues serve as "coordinates" for ligand orientation in the binding pocket of inhibitory ligand-gated ion channels.

Glycine is not only the principle agonist of the GlyR but also an essential coagonist of the NMDAR. Although both receptors depend on glycine for efficient channel activation, their glycine binding sites differ in structural organization, antagonist pharmacology, and preference for amino acid stereoisomers (Pullan and Powel, 1992). Mutagenesis studies and crystallography have shown that the α-carboxyl and α-amino groups of glycine interact with arginine (R505) and aspartate (D714) residues located in distinct lobes of the glycine binding pocket formed by the NR1 subunit of the NMDAR (Furukawa and Gouaux, 2003; Hirai et al., 1996; Laube et al., 1997). Thus, crucial determinants of glycine binding to the NMDAR are similar to those in the GlyR and are equally located at opposite sides of a protein interface.

Determinants of Agonist and Antagonist Action

Strychnine is a competitive antagonist of the GlyR that also binds to the interface of adjacent subunits. At the + side, high-affinity strychnine binding to homooligomeric α1 GlyRs required the conserved glutamate E157, which is crucial for stabilizing glycine's α-amino group. At the − side, strychnine binding was most strongly affected upon substitution of α1R131, a residue that only marginally contributes to glycine binding. Thus, agonists and antagonists share overlapping but not identical binding determinants at the α1 GlyR. A different situation was found for the heterooligomeric receptor, where strychnine binding was mainly affected upon substituting βE180 at the +, and α1R131 at the −, sides of the interface. However, although these charged residues are conserved on the α1 + and on the β − side, the respective mutations did not affect strychnine binding, consistent with a preferential interaction of strychnine with the βα interface. This contrasts our findings with glycine, which does not discriminate between subunit interfaces of the heteromeric GlyR. Whether this may reflect different contributions of the α and β subunits to channel opening, as suggested in case of the nAChR (Unwin et al., 2002), is not clear presently.

For the nAChR, Unwin and colleagues have proposed a "sliding subunit" mechanism of channel opening that postulates extensive conformational changes resulting from agonist binding (Unwin et al., 2002). A recent study by Celie et al. (2004), however, reports that the X-ray structures of the agonist- and antagonist-ligated AChBP differ only modestly. Thus, subtle conformational rearrangements of the extracellular domains may be sufficient for channel opening. Following this concept, we speculate that the different functional consequences resulting from binding either agonist (glycine) or antagonist (strychnine) might reflect differences in the strengthening of subunit-subunit interactions (Laube et al., 2002). Furthermore, our previous modeling predicts that, at the GlyR, the modulatory effects of Zn^{2+} on agonist-triggered ion flux are due to binding of the

metal ion at subunit interfaces (Laube et al., 2002). In conclusion, modulation of subunit-subunit interactions appears to be a general mechanism for regulating state transitions within the Cys-loop receptor family.

Subunit Stoichiometry of Heterooligomeric GlyRs
The observation that at heterooligomeric GlyRs both the αβ and βα interfaces contribute to glycine binding has important implications for our understanding of GlyR function. GlyR channel opening has been reported to require the binding of >2 glycine molecules, as deduced from detailed kinetic analysis (Beato et al., 2002; Colquhoun and Sivilotti, 2004; Laube et al., 2000). Here, coexpression of mutant α1 with wt β subunits resulted in a full rescue of the EC_{50} value of glycine, whereas coexpression of the wt α1 subunit with the respective homologous β mutants produced a decrease in glycine apparent affinity. This was an indication that in heteromeric GlyRs the β subunit might contribute more importantly to glycine binding than the α1 subunit, and hence the α1:β stoichiometry might be 2:3 instead of 3:2 as previously determined (Burzomato et al., 2003; Langosch et al., 1988). Our experiments with the $(αβ)_T$ tandem construct lend further support to this idea. When expressed alone, $(αβ)_T$ failed to produce detectable channel activity, whereas coexpression with the β subunit, but not two low-affinity α1 mutants, generated functional heterooligomeric GlyRs. Again, this result is most easily reconciled with two copies of $(αβ)_T$ coassembling with β into a GlyR pentamer. This conclusion is confirmed further by our biochemical data. Upon metabolic labeling with $[^{35}S]$methionine followed by affinity purification of the recombinant α1β GlyR, the ratio of α1 and β subunit radioactivities was found to be very close to that predicted for an α1:β stoichiometry of 2:3. Furthermore, radioactivity ratios proved to be invariant regardless whether surface biotinylated, i.e., plasma membrane bound, or total GlyRs were affinity purified. In conclusion, all data presented here are consistent with the revised stoichiometry of 2α1:3β. The latter implies the formation of at least one ββ interface, as originally suggested from cross-linking experiments (Langosch et al., 1988). This unique interface might constitute a pharmacological target side on heteromeric GlyRs, in analogy to the αγ interface of GABA_ARs, which determines benzodiazepine pharmacology (Cromer et al., 2002).

The discrepancy between the subunit stoichiometry of heterooligomeric GlyRs determined here (2α1:3β) and that reported in previous studies (3α1:2β) cannot be attributed to variations in the β subunit content of recombinant GlyRs. Although the α1 and α2 subunits can coassemble into functional GlyRs at variable subunit ratios, incorporation of the β subunit has been shown to occur only at an invariant α:β subunit stoichiometry (Kuhse et al., 1993). In case of our cross-linking experiments with affinity-purified GlyR (Langosch et al., 1988), the formation of higher-order α subunit adducts may have been due to copurification of homooligomeric GlyRs that are present in significant amounts even in adult tissue (Chattipakorn and McMahon, 2002). Similarly, conclusions from glycine dose-response analyses of recombinant heteromeric mutant GlyRs (Burzo-

mato et al., 2003; Kuhse et al., 1993) are biased by uncertainties about the contribution of simultaneously formed homomeric receptors to the respective agonist-induced currents.

Our identification of the β subunit as the major polypeptide of heteromeric gephyrin binding, i.e., synaptic GlyRs (Meyer et al., 1995) sheds new light on the abundant and widespread expression of the *Glrb* gene in the embryonic and adult mammalian CNS (Fujita et al., 1991; Malosio et al., 1991). Previously, the presence of GlyR β transcripts in brain regions known to lack strychnine binding sites has been interpreted as evidence for the existence of yet unknown strychnine-insensitive GlyR or GABA_AR subtypes (Betz, 1991; Malosio et al., 1991). Now, we propose that the *Glrb* gene encoding the major ligand binding subunit of synaptic GlyRs is widely expressed, and that the assembly of functional GlyRs is regulated by the developmentally and neuronal subtype-specific synthesis of selected GlyR α subunits. This proposal is in line with the observation that GlyR α1 and α2 mRNAs are found dendritically on membrane cisternae, which are located beneath gephyrin-positive postsynaptic membrane specializations (Racca et al., 1997). As these subsynaptic GlyR transcripts have been implicated in synapse-specific and/or activity-regulated translation processes, heterooligomeric GlyR assembly at synaptic sites may be controlled by local α but not β mRNA pools. Furthermore, the revised subunit stoichiometry deduced here may also be relevant for GlyR anchoring to the postsynaptic scaffolding protein gephyrin (Kneussel and Betz, 2000). Gephyrin is a highly mosaic protein that carries a binding site for the cytoplasmatic loop of the β subunit on its C-terminal E domain (Sola et al., 2004). Notably, native gephyrin is a trimer (Sola et al., 2001; Sola et al., 2004). Hence, the three β loop sequences present in the GlyR pentamer may interact with up to three E domains of gephyrin and thereby allow for distinct kinetic states of GlyR immobilization on the subsynaptic gephyrin lattice (Dahan et al., 2003).

Pathological Implications
Mutations in GlyR genes cause hereditary neuromotor diseases in man and animals (Schofield, 2002). Specifically, amino acid substitutions in the α1 subunit have been identified in patients suffering from dominant and recessive forms of hereditary hyperekplexia (or startle disease). Related mouse mutants have been shown to be deficient in either GlyR α1 or β subunit function. The mutant *spastic* (*spa*) has an intronic insertion of a repetitive element in the *Glrb* gene that leads to inefficient processing of the β pre-mRNA, and hence strongly reduced levels of β subunit protein (Kingsmore et al., 1994; Mulhardt et al., 1994). Consistent with this insertion being causal for the disease phenotype, *spa* mice have been rescued by a rat β subunit transgene (Hartenstein et al., 1996). Recently, a human startle disease phenotype has been associated with a missense mutation in *Glrb* that reduces the apparent affinity of heteromeric GlyRs (Rees et al., 2002). This mutation causes a 3.4-fold increase in the EC_{50} for glycine compared to wt α1β GlyR. The data presented here suggest that yet unclassified forms of hyperekplexia may in-

volve other mutations in the human *Glrb* gene, which directly affect ligand binding to αβ or βα subunit interfaces.

Experimental Procedures

Expression of Mutant GlyRs and Electrophysiological Recording

Mutations were introduced into the human α1 and β subunit cDNAs subcloned in the pNKS2 vector by using the QuikChange Site-Directed Mutagenesis Kit (Stratagene). All substitutions were confirmed by DNA sequencing. cRNAs of mutant and wt GlyRs were synthesized and injected as described previously (Laube et al., 2000). For the expression of heterooligomeric GlyRs, a α1:β cRNA ratio of 1:4 was used. Two-electrode voltage-clamp recording of whole-cell currents was performed in Ringer's solution (Laube et al., 2000) at a holding potential of −70 mV (or −40 mV at high expression levels). Dose-response curves for the agonists glycine and taurine were generated by measuring the inward current elicited by increasing agonist concentrations, whereas antagonist inhibition curves were obtained by coapplying glycine at a concentration corresponding to the respective EC_{50} value with increasing concentrations of the antagonist strychnine. For data analysis, agonist-induced peak currents (I) were normalized to the maximal current value (I_{max}) and fitted with the Hill equation as described (Wittekindt et al., 2001). To determine half-maximal effective antagonist concentrations (IC_{50}) from inhibition curves, results were fitted by the following equation: $I = I_{max}((1/B)^{n_H}/((1/B)^{n_H} + (1/C)^{n_H}))$, where I corresponds to the current obtained, I_{max} corresponds to the maximal agonist-induced current, B corresponds to the concentration of the antagonist, and n_H corresponds to the Hill coefficient. Experimental values are presented as the mean ± SD of peak current responses; significant differences were identified by Student's t test.

Molecular Modeling of GlyR N-Terminal Domains

Molecular modeling was done by using the SYBYL 6.9 program (Tripos Associates, St Louis, MI). The sequence alignment of the extracellular domains of the GlyR α1 and β subunits with AChBP was taken from Brejc et al. (2001) and used with some minor changes (see Figure 1A). Based on the crystal structure of AChBP (Brejc et al., 2001); Brookhaven Protein Data Bank entry 1I9B), we constructed the Cα framework of GlyR α1 and β subunits by using structurally conserved regions (SCRs), which mainly correspond to the α helices and β sheets of the AChBP structure. However, in the very N-terminal region the α helix present in AChBP was aligned to the SDFLDKL sequence of the GlyR α1 subunit, in agreement with the hydrophobic residues FL..L. and IL..I, respectively. Missing peptide fragments were then extracted from the Sybyl Protein Database within COMPOSER and joined to the SCRs. The following operations were performed by using the Tripos force field and Kollman all-atom charges. After addition of all hydrogen atoms, the resulting structure was subjected to molecular dynamic (MD) simulation runs (NTV ensemble, 300 K) for 100 to 1000 fs and energy minimized in the absence of solvent (Powell method; gradient 0.1 kcal/mol * A). This procedure was repeated until a minimum in energy was reached. Then, the respective ligands were introduced into the binding pocket of the wt receptor by positioning them ideally with the help of DOCK in a conformation that closely matched that of the ligands bound in AChBP (Celie et al., 2004). The individual ligand protein complexes were subjected to MD simulation in Sybyl (version 6.9) using the TRIPOS force field to achieve optimal configuration for up to 100 fs. In case of alternative docking conformations, the energetically lowest was chosen. To produce the final structures, the MD was subsequently minimized with the Powell algorithm until an energy gradient of 0.01 kcal/mol was reached. The resulting structures were used to evaluate changes in binding site interactions caused by mutation of binding site residues.

Construction of a Tandem α1β cDNA

A concatemeric GlyR polypeptide encompassing the human α1 and β subunits, $(αβ)_T$, was generated by expressing a tandem cDNA subcloned into the pNKS2 vector. In this construct, the C terminus of the α1 subunit was connected to the N terminus of the β subunit via a linker consisting of a 7-fold Ala-Gly-Ser repeat encoded by

the nucleotide sequence (GCT GGA AGT) (Zhou et al., 2003). The α1 subunit cDNA in the pNKS2 vector was digested with the restriction enzymes AatII and NotI, resulting in a loss of the last four amino acids at the C terminus. The β subunit cDNA insert was excised from the pNKS4 vector with the restriction enzymes BbsI and NotI, thereby deleting the signal peptide and the first amino acid. The missing nucleotides were restored within the linker flanked by an AatII site at the 5′ and a BbsI restriction site at the 3′ end of the coding sequence. Finally, both the linker and the β subunit cDNA were ligated into the α1 pNKS2 vector sequence.

Subunit Composition of Metabolically Labeled α1β GlyRs

For the biochemical determination of subunit stoichiometry, oocytes coinjected with wt α1 or His-tagged α1 and His-tagged β subunit cRNAs at a ratio of 1:4 were metabolically labeled by overnight incubation with [³⁵S]methionine as described previously (Sadtler et al., 2003). After an additional 24 hr chase interval, a digitonin (1% [w/v]; Sigma-Aldrich, München, Germany) extract was prepared, and GlyRs were natively purified by Ni^{2+}-NTA chromatography as described (Nicke et al., 1998).

For isolating plasma membrane bound α1β GlyRs, oocytes coinjected with wt α1 and His-tagged β subunit cRNAs (ratio 1:4) and metabolically labeled as detailed above were chased with 10 mM methionine for 36 hr and then exposed for 30 min at ambient temperature to the cleavable biotinylation reagent sulfo-NHS-SS-biotin (Pierce, Bonn, Germany) at 10 mg/ml in oocyte phosphate-buffered saline (PBS) (30 mM phosphate, 110 mM NaCl, 1 mM $CaCl_2$, 1 mM $MgCl_2$ [pH 8.0]). Biotinylated cells were washed in oocyte PBS and lysed in phosphate buffer (0.1 M [pH 8.0]), containing dodecylmaltoside (0.2% [w/v]; Calbiochem, Schwalbach/Taunus, Germany) and 50 mM iodoacetamide, and α1β complexes were natively purified via the His-tagged β subunit by Ni^{2+}-NTA affinity chromatography. Bound α1β complexes were released by two subsequent incubations, each for 15 min at 37°C, with modified RIPA buffer (1% NP40, 0.5% deoxycholic acid, 0.1% SDS, 150 mM NaCl, 10 mM EDTA) supplemented with 250 mM imidazole-HCl (pH 7.2). After 5-fold dilution with phosphate buffer, biotinylated α1 and His-tagged β subunits were captured by incubation overnight at 4°C with ImmunoPure Immobilized Streptavidin (Pierce, Bonn, Germany), followed by washing of the resin with 0.2% dodecylmaltoside in phosphate buffer. Bound proteins were released by incubation for 5 min at 95°C in SDS sample buffer containing 50 mM dithiothreitol (DTT).

The purified GlyR was separated on 10% SDS-PAGE gels, which were fixed, dried, and exposed to PhosphorImager screens. The radioactivity of individual polypeptide bands was quantified using a PhosphorImager (Molecular Dynamics) and evaluated using the software package ImageQuant.

References

Beato, M., Groot-Kormelink, P.J., Colquhoun, D., and Sivilotti, L.G. (2002). Openings of the rat recombinant alpha 1 homomeric glycine receptor as a function of the number of agonist molecules bound. J. Gen. Physiol. *119*, 443–466.

Becker, C.M. (1992). Convulsants acting at the inhibitory glycine receptor. In Handbook of Experimental Pharmacology, H. Herken and F. Hucho, eds. (Heidelberg, Germany: Springer), pp. 539–575.

Betz, H. (1991). Glycine receptors: heterogeneous and widespread in the mammalian brain. Trends Neurosci. *14*, 458–461.

Bormann, J., Rundstrom, N., Betz, H., and Langosch, D. (1993). Residues within transmembrane segment M2 determine chloride conductance of glycine receptor homo- and hetero-oligomers. EMBO J. *12*, 3729–3737.

Breitinger, H.G., and Becker, C.M. (2002). The inhibitory glycine receptor—simple views of a complicated channel. ChemBioChem *3*, 1042–1052.

Brejc, K., van Dijk, W.J., Klaassen, R.V., Schuurmans, M., van Der Oost, J., Smit, A.B., and Sixma, T.K. (2001). Crystal structure of an ACh
-binding protein reveals the ligand-binding domain of nicotinic receptors. Nature *411*, 269–276.

Burzomato, V., Groot-Kormelink, P.J., Sivilotti, L.G., and Beato, M. (2003). Stoichiometry of recombinant heteromeric glycine receptors revealed by a pore-lining region point mutation. Receptors Channels *9*, 353–361.

Büttner, C., Sadtler, S., Leyendecker, A., Laube, B., Griffon, N., Betz, H., and Schmalzing, G. (2001). Ubiquitination precedes internalization and proteolytic cleavage of plasma membrane-bound glycine receptors. J. Biol. Chem. *276*, 42978–42985.

Celie, P.H., van Rossum-Fikkert, S.E., van Dijk, W.J., Brejc, K., Smit, A.B., and Sixma, T.K. (2004). Nicotine and carbamylcholine binding to nicotinic acetylcholine receptors as studied in AChBP crystal structures. Neuron *41*, 907–914.

Chattipakorn, S.C., and McMahon, L.L. (2002). Pharmacological characterization of glycine-gated chloride currents recorded in rat hippocampal slices. J. Neurophysiol. *87*, 1515–1525.

Colquhoun, D. (1998). Binding, gating, affinity and efficacy: the interpretation of structure-activity relationships for agonists and of the effects of mutating receptors. Br. J. Pharmacol. *125*, 924–947.

Colquhoun, D., and Sivilotti, L.G. (2004). Function and structure in glycine receptors and some of their relatives. Trends Neurosci. *27*, 337–344.

Corringer, P.J., Le Novere, N., and Changeux, J.P. (2000). Nicotinic receptors at the amino acid level. Annu. Rev. Pharmacol. Toxicol. *40*, 431–458.

Cromer, B.A., Morton, C.J., and Parker, M.W. (2002). Anxiety over GABA(A) receptor structure relieved by AChBP. Trends Biochem. Sci. *27*, 280–287.

Cull-Candy, S., Brickley, S., and Farrant, M. (2001). NMDA receptor subunits: diversity, development and disease. Curr. Opin. Neurobiol. *11*, 327–335.

Dahan, M., Levi, S., Luccardini, C., Rostaing, P., Riveau, B., and Triller, A. (2003). Diffusion dynamics of glycine receptors revealed by single-quantum dot tracking. Science *302*, 442–445.

Fujita, M., Sato, K., Sato, M., Inoue, T., Kozuka, T., and Tohyama, M. (1991). Regional distribution of the cells expressing glycine receptor beta subunit mRNA in the rat brain. Brain Res. *560*, 23–37.

Furukawa, H., and Gouaux, E. (2003). Mechanisms of activation, inhibition and specificity: crystal structures of the NMDA receptor NR1 ligand-binding core. EMBO J. *22*, 2873–2885.

Grutter, T., and Changeux, J.P. (2001). Nicotinic receptors in wonderland. Trends Biochem. Sci. *26*, 459–463.

Hartenstein, B., Schenkel, J., Kuhse, J., Besenbeck, B., Kling, C., Becker, C.M., Betz, H., and Weiher, H. (1996). Low level expression of glycine receptor beta subunit transgene is sufficient for phenotype correction in spastic mice. EMBO J. *15*, 1275–1282.

Harvey, R.J., Depner, U.B., Wassle, H., Ahmadi, S., Heindl, C., Reinold, H., Smart, T.G., Harvey, K., Schutz, B., Abo-Salem, O.M., et al. (2004). GlyR alpha3: an essential target for spinal PGE2-mediated inflammatory pain sensitization. Science *304*, 884–887.

Hirai, H., Kirsch, J., Laube, B., Betz, H., and Kuhse, J. (1996). The glycine binding site of the N-methyl-D-aspartate receptor subunit NR1: identification of novel determinants of co-agonist potentiation in the extracellular M3–M4 loop region. Proc. Natl. Acad. Sci. USA *93*, 6031–6036.

Kingsmore, S.F., Giros, B., Suh, D., Bieniarz, M., Caron, M.G., and Seldin, M.F. (1994). Glycine receptor beta-subunit gene mutation in

spastic mouse associated with LINE-1 element insertion. Nat. Genet. *7*, 136–141.

Kneussel, M., and Betz, H. (2000). Clustering of inhibitory neurotransmitter receptors at developing postsynaptic sites: the membrane activation model. Trends Neurosci. *23*, 429–435.

Kuhse, J., Laube, B., Magalei, D., and Betz, H. (1993). Assembly of the inhibitory glycine receptor: identification of amino acid sequence motifs governing subunit stoichiometry. Neuron *11*, 1049–1056.

Kuhse, J., Betz, H., and Kirsch, J. (1995). The inhibitory glycine receptor: architecture, synaptic localization and molecular pathology of a postsynaptic ion-channel complex. Curr. Opin. Neurobiol. *5*, 318–323.

Langosch, D., Thomas, L., and Betz, H. (1988). Conserved quaternary structure of ligand-gated ion channels: the postsynaptic glycine receptor is a pentamer. Proc. Natl. Acad. Sci. USA *85*, 7394–7398.

Laube, B., Hirai, H., Sturgess, M., Betz, H., and Kuhse, J. (1997). Molecular determinants of agonist discrimination by NMDA receptor subunits: analysis of the glutamate binding site on the NR2B subunit. Neuron *18*, 493–503.

Laube, B., Kuhse, J., and Betz, H. (2000). Kinetic and mutational analysis of Zn2+ modulation of recombinant human inhibitory glycine receptors. J. Physiol. *522*, 215–230.

Laube, B., Maksay, G., Schemm, R., and Betz, H. (2002). Modulation of glycine receptor function: a novel approach for therapeutic intervention at inhibitory synapses? Trends Pharmacol. Sci. *23*, 519–527.

Legendre, P. (2001). The glycinergic inhibitory synapse. Cell. Mol. Life Sci. *58*, 760–793.

Le Novere, N., Grutter, T., and Changeux, J.P. (2002). Models of the extracellular domain of the nicotinic receptors and of agonist- and Ca2+-binding sites. Proc. Natl. Acad. Sci. USA *99*, 3210–3215.

Maksay, G., Bikadi, Z., and Simonyi, M. (2003). Binding interactions of antagonists with 5-hydroxytryptamine3A receptor models. J. Recept. Signal Transduct. Res. *23*, 255–270.

Malosio, M.L., Marqueze-Pouey, B., Kuhse, J., and Betz, H. (1991). Widespread expression of glycine receptor subunit mRNAs in the adult and developing rat brain. EMBO J. *10*, 2401–2409.

Meyer, G., Kirsch, J., Betz, H., and Langosch, D. (1995). Identification of a gephyrin binding motif on the glycine receptor beta subunit. Neuron *15*, 563–572.

Mulhardt, C., Fischer, M., Gass, P., Simon-Chazottes, D., Guenet, J.L., Kuhse, J., Betz, H., and Becker, C.M. (1994). The spastic mouse: aberrant splicing of glycine receptor beta subunit mRNA caused by intronic insertion of L1 element. Neuron *13*, 1003–1015.

Nicke, A., Baumert, H.G., Rettinger, J., Eichele, A., Lambrecht, G., Mutschler, E., and Schmalzing, G. (1998). P2X1 and P2X3 receptors form stable trimers: a novel structural motif of ligand-gated ion channels. EMBO J. *17*, 3016–3028.

Pfeiffer, F., Graham, D., and Betz, H. (1982). Purification by affinity chromatography of the glycine receptor of rat spinal cord. J. Biol. Chem. *257*, 9389–9393.

Pribilla, I., Takagi, T., Langosch, D., Bormann, J., and Betz, H. (1992). The atypical M2 segment of the beta subunit confers picrotoxinin resistance to inhibitory glycine receptor channels. EMBO J. *11*, 4305–4311.

Pullan, L.M., and Powel, R.J. (1992). Comparison of binding at strychnine-sensitive (inhibitory glycine receptor) and strychnine-insensitive (N-methyl-D-aspartate receptor) glycine binding sites. Neurosci. Lett. *148*, 199–201.

Racca, C., Gardiol, A., and Triller, A. (1997). Dendritic and postsynaptic localizations of glycine receptor alpha subunit mRNAs. J. Neurosci. *17*, 1691–1700.

Rajendra, S., Vandenberg, R.J., Pierce, K.D., Cunningham, A.M., French, P.W., Barry, P.H., and Schofield, P.R. (1995). The unique extracellular disulfide loop of the glycine receptor is a principal ligand binding element. EMBO J. *14*, 2987–2998.

Rajendra, S., Lynch, J.W., and Schofield, P.R. (1997). The glycine receptor. Pharmacol. Ther. *73*, 121–146.

Rees, M.I., Lewis, T.M., Kwok, J.B., Mortier, G.R., Govaert, P., Snell, R.G., Schofield, P.R., and Owen, M.J. (2002). Hyperekplexia associated with compound heterozygote mutations in the beta-subunit of the human inhibitory glycine receptor (GLRB). Hum. Mol. Genet. *11*, 853–860.

Sadtler, S., Laube, B., Lashub, A., Nicke, A., Betz, H., and Schmalzing, G. (2003). A basic cluster determines topology of the cytoplasmic M3–M4 loop of the glycine receptor alpha1 subunit. J. Biol. Chem. *278*, 16782–16790.

Schmieden, V., Kuhse, J., and Betz, H. (1993). Mutation of glycine receptor subunit creates beta-alanine receptor responsive to GABA. Science *262*, 256–258.

Schofield, P.R. (2002). The role of glycine and glycine receptors in myoclonus and startle syndromes. Adv. Neurol. *89*, 263–274.

Singer, J.H., and Berger, A.J. (2000). Development of inhibitory synaptic transmission to motoneurons. Brain Res. Bull. *53*, 553–560.

Sixma, T.K., and Smit, A.B. (2003). Acetylcholine binding protein (AChBP): a secreted glial protein that provides a high-resolution model for the extracellular domain of pentameric ligand-gated ion channels. Annu. Rev. Biophys. Biomol. Struct. *32*, 311–334.

Sola, M., Kneussel, M., Heck, I.S., Betz, H., and Weissenhorn, W. (2001). X-ray crystal structure of the trimeric N-terminal domain of gephyrin. J. Biol. Chem. *276*, 25294–25301.

Sola, M., Bavro, V.N., Timmins, J., Franz, T., Ricard-Blum, S., Schoehn, G., Ruigrok, R.W., Paarmann, I., Saiyed, T., O'Sullivan, G.A., et al. (2004). Structural basis of dynamic glycine receptor clustering by gephyrin. EMBO J. *23*, 2510–2519.

Takahashi, T., Momiyama, A., Hirai, K., Hishinuma, F., and Akagi, H. (1992). Functional correlation of fetal and adult forms of glycine receptors with developmental changes in inhibitory synaptic receptor channels. Neuron *9*, 1155–1161.

Unwin, N. (2003). Structure and action of the nicotinic acetylcholine receptor explored by electron microscopy. FEBS Lett. *555*, 91–95.

Unwin, N., Miyazawa, A., Li, J., and Fujiyoshi, Y. (2002). Activation of the nicotinic acetylcholine receptor involves a switch in conformation of the alpha subunits. J. Mol. Biol. *319*, 1165–1176.

Vandenberg, R.J., French, C.R., Barry, P.H., Shine, J., and Schofield, P.R. (1992a). Antagonism of ligand-gated ion channel receptors: two domains of the glycine receptor alpha subunit form the strychnine-binding site. Proc. Natl. Acad. Sci. USA *89*, 1765–1769.

Vandenberg, R.J., Handford, C.A., and Schofield, P.R. (1992b). Distinct agonist- and antagonist-binding sites on the glycine receptor. Neuron *9*, 491–496.

Wittekindt, B., Malany, S., Schemm, R., Otvos, L., Maccecchini, M.L., Laube, B., and Betz, H. (2001). Point mutations identify the glutamate binding pocket of the N-methyl-D-aspartate receptor as major site of conantokin-G inhibition. Neuropharmacology *41*, 753–761.

Zhou, Y., Nelson, M.E., Kuryatov, A., Choi, C., Cooper, J., and Lindstrom, J. (2003). Human alpha4beta2 acetylcholine receptors formed from linked subunits. J. Neurosci. *23*, 9004–9015.

Zoghbi, H.Y., Gage, F.H., and Choi, D.W. (2000). Neurobiology of disease. Curr. Opin. Neurobiol. *10*, 655–660.